

**Zeitschrift:** Schweizerische mineralogische und petrographische Mitteilungen = Bulletin suisse de minéralogie et pétrographie  
**Band:** 51 (1971)  
**Heft:** 2-3  
  
**Artikel:** A study of inherited and newly formed zircons from paragneisses and granitised sediments of the Strona-Ceneri-Zone (Southern Alps)  
**Autor:** Köppel, V. / Grünenfelder, M.  
**DOI:** <https://doi.org/10.5169/seals-39827>

### **Nutzungsbedingungen**

Die ETH-Bibliothek ist die Anbieterin der digitalisierten Zeitschriften auf E-Periodica. Sie besitzt keine Urheberrechte an den Zeitschriften und ist nicht verantwortlich für deren Inhalte. Die Rechte liegen in der Regel bei den Herausgebern beziehungsweise den externen Rechteinhabern. Das Veröffentlichen von Bildern in Print- und Online-Publikationen sowie auf Social Media-Kanälen oder Webseiten ist nur mit vorheriger Genehmigung der Rechteinhaber erlaubt. [Mehr erfahren](#)

### **Conditions d'utilisation**

L'ETH Library est le fournisseur des revues numérisées. Elle ne détient aucun droit d'auteur sur les revues et n'est pas responsable de leur contenu. En règle générale, les droits sont détenus par les éditeurs ou les détenteurs de droits externes. La reproduction d'images dans des publications imprimées ou en ligne ainsi que sur des canaux de médias sociaux ou des sites web n'est autorisée qu'avec l'accord préalable des détenteurs des droits. [En savoir plus](#)

### **Terms of use**

The ETH Library is the provider of the digitised journals. It does not own any copyrights to the journals and is not responsible for their content. The rights usually lie with the publishers or the external rights holders. Publishing images in print and online publications, as well as on social media channels or websites, is only permitted with the prior consent of the rights holders. [Find out more](#)

**Download PDF:** 19.07.2025

**ETH-Bibliothek Zürich, E-Periodica, <https://www.e-periodica.ch>**

# **A Study of Inherited and Newly Formed Zircons from Paragneisses and Granitised Sediments of the Strona-Ceneri-Zone (Southern Alps)**

By *V. Köppel* and *M. Grünenfelder* (Zürich)\*)

With 9 figures and 5 tables in the text

## **Abstract**

Concordant,  $450 \pm 10$  my old monazite dates the regional amphibolite facies metamorphism within the Strona-Ceneri zone of the Southern Alps.

Zircons of granitic gneisses which appear to be the product of an anatectic in situ granitisation of sediments that accompanied the amphibolite facies metamorphism yielded almost concordant ages of 430–500 my. Equally concordant ages were obtained from zircons in rocks that were partially granitised by metasomatism, and in neighbouring paragneisses up to 100 m away from granitised rocks.

The comparably high trace element content of these zircon suites, their morphological properties, and their disturbed crystal lattice are interpreted to be indicative of new zircon growth during the granitisation process.

In contrast, zircon suites from paragneisses showing no signs of granitisation have highly discordant apparent ages (560–1880 my). These zircons have a low trace element content and variable morphologies. Their relatively undisturbed crystal lattice indicates that they were annealed and partly recrystallised during the amphibolite facies metamorphism that accompanied the local granitisation process.

From the apparent ages of the paragneiss zircons it is concluded that the oldest population is older than 2500 my. From the Rb-Sr data of a rock unit within the Austro-Alpine nappes showing similarities with the crystalline basement of the Southern Alps it is tentatively concluded that the basement of the Southern Alps was also formed during the Caledonian orogeny.

Zircons of an aplitic alkali-feldspar-gneiss from the neighbouring Val Colla zone consist, according to their X-ray powder diffraction pattern, of two zircon phases. The apparent ages range from 140–580 my. The discordant age pattern is probably due to the presence of these two phases.

---

\*) Institute for Crystallography and Petrology, Swiss Federal Institute of Technology, Sonneggstrasse 3, CH-8006 Zürich.

### Zusammenfassung

Die konkordanten U-Pb-Alterswerte von  $450 \pm 10$  Mio. J. einer Monazitprobe aus einem Paragneis der Strona-Ceneri-Zone datieren die regionale Amphibolitfazies-Metamorphose.

Zirkone aus granitischen Gneisen, welche vermutlich aus einer anatektischen In-situ-Granitisation von Sedimenten entstanden sind, ergaben fast konkordante U-Pb-Alterswerte von 430–500 Mio. J. und weisen auf einen engen zeitlichen Zusammenhang der kaledonischen Metamorphose der Amphibolitfazies mit der Granitisierung hin. Ähnlich konkordante Alterswerte ergaben Zirkone aus Mischgneisen und aus benachbarten Paragneisen.

Der relativ hohe Gehalt dieser Zirkone an Spurenelementen, ihre Morphologie und ihr durch Domänenbau gestörtes Kristallgitter deuten darauf hin, dass die Zirkone während der Granitisierung neu gebildet wurden. Die neugebildeten Zirkone finden sich ausschliesslich in Kalifeldspat führenden Gesteinen.

Im Gegensatz dazu enthalten die Kalifeldspat-freien Paragneise Zirkone mit stark diskordanten, präkambrischen Altern (560–1880 Mio. J.). Das wenig gestörte Kristallgitter zeigt, dass die Zirkone rekristallisierten, z. T. unter Beibehaltung des während des Sedimentationszyklus entstandenen gerundeten Habitus, z. T. aber auch unter Bildung von neuen Kristallflächen. Diese idiomorphen Kristalle weisen einen anderen Habitus auf als die bei der Granitisierung entstandenen. Sie treten entweder für sich allein, oder zusammen mit gerundeten Zirkonen auf. Beide Typen weisen denselben niedrigen Gehalt an Spurenelementen auf und ergaben ähnliche Zerfallsalter.

Das Minimalalter der ältesten Population der detritischen Zirkonmischung der Paragneise beträgt 2500 Mio. J.

Die Zerfallsalter von Zirkonen des aplitischen Alkalifeldspatgneises (Gneis Chiari) der Val-Colla-Zone sind stark diskordant (138–580 Mio. J.). Pulveraufnahmen ergaben die Anwesenheit von zwei verschiedenen Zirkonphasen. Die Morphologie, der hohe Spurenelementgehalt und das gestörte Gitter deuten im Vergleich zu den Beobachtungen in der Ceneri-Zone darauf hin, dass es sich nicht um detritische Zirkone, sondern um Zirkonneubildungen im Gneis Chiari handelt.

### 1. INTRODUCTION

In the Strona-Ceneri zone of the Southern Alps (fig. 1), that underwent an amphibolite facies metamorphism accompanied by local in situ granitisation geochronological work has already been performed by PIDGEON et al. (1970) and McDOWELL (1970).

PIDGEON et al. reported almost concordant zircon U-Pb ages (430–465 my) from a potassium-feldspar-bearing biotite-plagioclase-gneiss. This rock type was formerly considered to represent an orthogneiss (KELTERBORN, 1927), whereas GRAETER (1951) and REINHARD (1964) believe this rock to be a granitised sediment.

From a neighbouring representative of the paragneiss series in the basement of the Strona-Ceneri zone PIDGEON et al. (1970) obtained strongly discordant U-Pb age patterns (670–959 my) indicating an apparent lead loss of 80–90%.

The authors concluded that the zircons in the granitic rock were almost completely reconstituted during a granitisation process, whereas the zircons of the paragneiss suffered only a drastic lead loss.

In this paper we report further information concerning the question of zircon reconstitution during a granitisation process. In addition to U-Pb age determinations of zircons their morphology was examined microscopically and the trace element contents and distributions of U, P, Y, and Ca were determined by microprobe techniques. Cell dimensions were determined by X-ray powder diffraction. These studies should reveal correlations indicative for the origin and history of the zircon suites.

McDOWELL (1970) reported K-Ar ages of biotite, muscovite and hornblende from the Strona-Ceneri and the neighbouring Val Colla zone. The author concluded from the concordant age cluster of the biotite-muscovite pair around 320 my that the amphibolite facies metamorphism is of Hercynian age. Higher, up to 390 my old hornblende ages are interpreted as being due to an incomplete Ar loss during the metamorphism. Towards the western part of the Strona-Ceneri zone the mica ages decrease, become discordant and reflect an event 180–200 my old.

To obtain additional information as to the time of the regional metamorphism monazite fractions from a paragneiss were analysed.

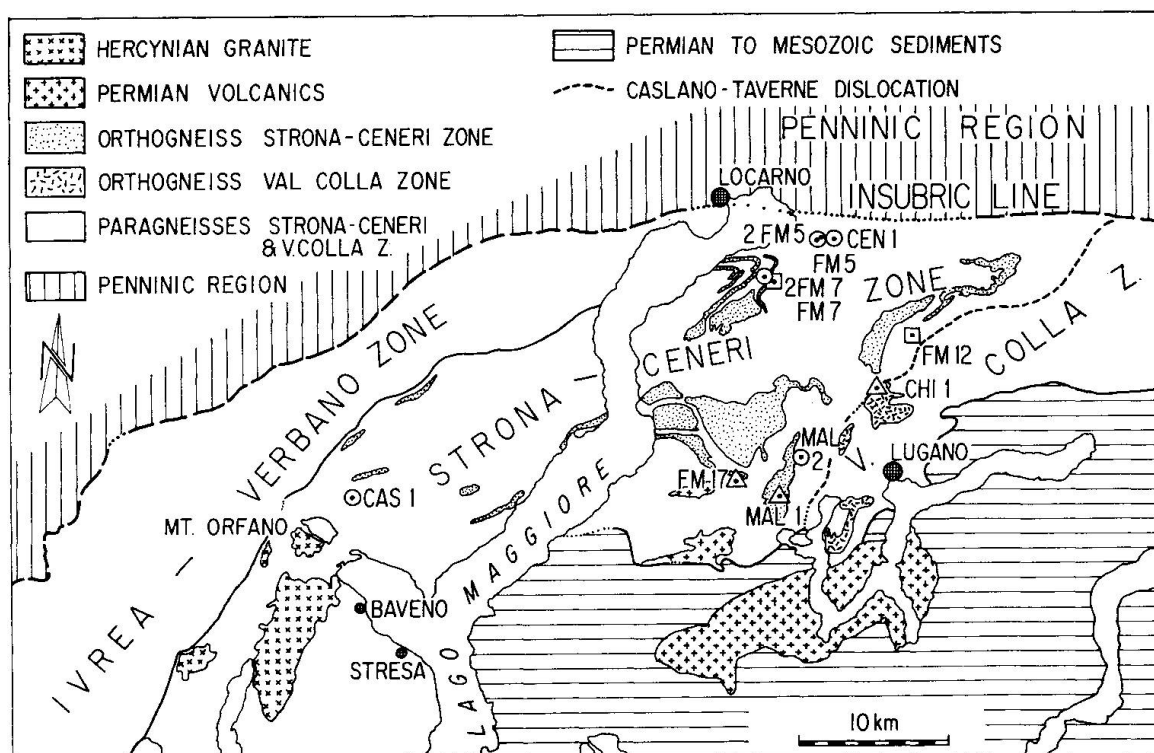


Fig. 1. Geological sketch map of the Southern Alps showing the sample locations.

Furthermore zircons from an aplitic alkali-feldspar-gneiss of the Val Colla zone were analysed to determine its age and to obtain information about its origin.

## 2. GEOLOGICAL AND PETROGRAPHIC SETTING

The geology of the Strona-Ceneri and the Val Colla zones have been discussed in detail by several authors: BÄCHLIN (1937), GRAETER (1951), REINHARD (1964), KÖPPEL (1966), and BORIANI (1968, 1970a, b, c).

Within the *Strona-Ceneri* zone two principal rock types occur, namely a biotite-plagioclase-gneiss and a K-feldspar-biotite-plagioclase-gneiss. The chemical compositions are listed according to REINHARD (1964) in table 1.

The biotite-plagioclase-gneiss varies widely in composition. Common varieties are hornblende-biotite-plagioclase-gneiss, biotite-muscovite-plagioclase-gneiss containing occasional garnet and kyanite, granulated biotite-plagioclase-gneiss with inclusions of lime silicates, and sillimanite-bearing biotite-plagioclase-gneiss. These varieties are considered to be paragneisses.

In contrast, the K-feldspar-biotite-plagioclase-gneiss (henceforth called granitic gneiss) is rather uniform in its mineralogical and chemical composition. Aplitic varieties are of minor importance. They form well defined, usually 10–20 m thick layers in paragneisses and transitional rock types (see below). In some places they change to conformable aplites or pegmatites.

Both the granitic gneisses and the paragneisses follow the same structural trends. No intrusive contacts are visible. Paragneisses adjacent to granitic gneisses contain K-feldspar; the K-feldspar content gradually increases towards the granitic gneiss, and thus characterises a transitional rock type. Such zones may reach widths of several 100 m. They commonly occur, together with paragneisses, as bands in granitic gneisses or form isolated layers in paragneisses.

These observations and the absence of migmatites point to an in situ granitisation of sediments.

The *Val Colla* zone, separated from the Strona-Ceneri zone by the Caslano-Taverne fault zone, the latest activity of which occurred between the upper Carboniferous and the Permian, differs in that this zone contains rocks of greenschist facies in tectonic contact with amphibolite facies rocks. K-feldspar-biotite-plagioclase gneisses are absent. The Chiari or Bernardo gneiss, an aplitic muscovite-alkali-feldspar-gneiss, is extensively brecciated and mylonitised. Its contact towards the phyllonites (paragneisses and schists) is tectonic. The origin of this aplitic gneiss is still debated (EL TAHLAWI, 1965). The rock is considered to represent either a metamorphic arkose or a granitic intrusion. According to GRAETER (1951) and REINHARD (1964), this rock is intrusive and has assimilated Al-rich metasediments.



Table 2. *Analytical data of zircons and monazite*

| Sample             | Size fractions<br>in microns | ppm U | ppm Th | ppm<br>rad. Pb | Observed ratios                      |                                      | Radiogenic Pb in % |                   |                   |
|--------------------|------------------------------|-------|--------|----------------|--------------------------------------|--------------------------------------|--------------------|-------------------|-------------------|
|                    |                              |       |        |                | Pb <sup>206</sup> /Pb <sup>204</sup> | Pb <sup>207</sup> /Pb <sup>204</sup> | Pb <sup>206</sup>  | Pb <sup>207</sup> | Pb <sup>208</sup> |
| Strona-Ceneri zone |                              |       |        |                |                                      |                                      |                    |                   |                   |
| <i>Group A</i>     |                              |       |        |                |                                      |                                      |                    |                   |                   |
| MAL 1*)            | 150-75                       | 1403  | —      | 94.9           | 1370                                 | 94.55                                | 89.94              | 5.267             | 4.793             |
| MAL 1              | 75-53                        | 1617  | —      | 107.1          | 1875                                 | 120.7                                | 89.51              | 5.080             | 5.412             |
| MAL 1              | 53-42                        | 1620  | —      | 107.0          | 1751                                 | 113.4                                | 89.19              | 5.048             | 5.758             |
| MAL 1              | -42                          | 1626  | —      | 108.1          | 1433                                 | 95.18                                | 89.00              | 5.025             | 5.974             |
| FM 17              | total fraction               | 1031  | —      | 70.0           | 1269                                 | 87.07                                | 89.29              | 5.125             | 5.584             |
| FM 7               | total fraction               | 1102  | —      | 81.0           | 2895                                 | 180.9                                | 90.52              | 5.211             | 4.274             |
| FM 12              | total fraction               | 1028  | —      | 76.2           | 973                                  | 68.96                                | 83.79              | 4.711             | 11.50             |
| <i>Group B</i>     |                              |       |        |                |                                      |                                      |                    |                   |                   |
| MAL 2*)            | 150-75 n. m.                 | 431   | —      | 58.0           | 1541                                 | 146.4                                | 83.02              | 7.145             | 9.838             |
| MAL 2              | 150-75 n. m.                 | 444   | —      | 59.2           | 1685                                 | 159.6                                | 82.89              | 7.174             | 9.938             |
| MAL 2              | 75-53 n. m.                  | 473   | —      | 62.1           | 1678                                 | 156.4                                | 83.36              | 7.085             | 9.550             |
| MAL 2              | 53-42 n. m.                  | 519   | —      | 64.7           | 1543                                 | 142.6                                | 84.12              | 7.020             | 8.862             |
| MAL 2              | -42 n. m.                    | 593   | —      | 69.4           | 1774                                 | 157.6                                | 84.78              | 6.869             | 8.355             |
| MAL 2              | 150-75 m.                    | 733   | —      | 85.0           | 1564                                 | 138.6                                | 84.22              | 6.715             | 9.066             |
| MAL 2              | 53-42 m.                     | 690   | —      | 80.8           | 1562                                 | 136.8                                | 84.45              | 6.643             | 8.907             |
| MAL 2              | -42 m.                       | 862   | —      | 95.6           | 1010                                 | 91.58                                | 84.59              | 6.505             | 8.900             |
| CEN 1              | +75 n. m.                    | 437   | —      | 68.7           | 835                                  | 107.5                                | 81.46              | 9.197             | 9.347             |
| CEN 1              | 75-53 n. m.                  | 516   | —      | 68.0           | 1462                                 | 158.0                                | 83.06              | 8.210             | 8.727             |
| CEN 1              | 53-42 n. m.                  | 567   | —      | 66.5           | 1772                                 | 175.9                                | 84.18              | 7.708             | 8.107             |
| CEN 1              | 53-42 m.                     | 590   | —      | 68.0           | 1078                                 | 110.8                                | 84.33              | 7.583             | 8.084             |
| CEN 1              | -42                          | 631   | —      | 66.8           | 1425                                 | 132.2                                | 84.76              | 7.046             | 8.197             |
| CAS 1              | +75 n. m.                    | 532   | 174    | 60.6           | 2837                                 | 241.5                                | 83.86              | 6.728             | 9.410             |
| CAS 1              | 75-53 n. m.                  | 610   | 186    | 63.9           | 1749                                 | 140.4                                | 84.87              | 6.132             | 8.995             |
| CAS 1              | 53-42 n. m.                  | 683   | 196    | 64.7           | 1056                                 | 87.42                                | 85.46              | 5.938             | 8.607             |
| CAS 1              | -42                          | 746   | 181    | 67.3           | 1364                                 | 105.2                                | 86.46              | 5.777             | 7.761             |
| CAS 1 Monazite     | total fraction               | 8361  | 37600  | 1230           | 1286                                 | 86.05                                | 56.59              | 2.722             | 40.69             |
| CAS 1 Monazite     | +75                          | 7980  | 37100  | 1256           | 5473                                 | 323.0                                | 58.28              | 2.228             | 39.49             |
| CAS 1 Monazite     | -42                          | 7940  | 34730  | 1229           | 3115                                 | 188.7                                | 56.74              | 2.294             | 40.97             |
| 2 FM 5             | +75 n. m.                    | 455   | —      | 57.7           | 1458                                 | 152.4                                | 83.39              | 7.940             | 8.674             |
| 2 FM 5             | 75-53 n. m.                  | 573   | —      | 60.6           | 804.3                                | 80.31                                | 84.81              | 7.003             | 8.190             |
| 2 FM 5             | 53-42 n. m.                  | 705   | —      | 64.0           | 832.5                                | 77.39                                | 86.21              | 6.573             | 7.220             |
| 2 FM 5             | -42                          | 718   | —      | 62.2           | 2045                                 | 163.0                                | 86.82              | 6.328             | 6.854             |

| Sample | Size fractions in microns | Atomic ratios | Apparent ages in my*)               |                                     |                                      |      |       | Atomic ratio | Apparent age |
|--------|---------------------------|---------------|-------------------------------------|-------------------------------------|--------------------------------------|------|-------|--------------|--------------|
|        |                           |               | Pb <sup>206</sup> /U <sup>238</sup> | Pb <sup>207</sup> /U <sup>235</sup> | Pb <sup>207</sup> /Pb <sup>206</sup> | 6/8  | 7/5   | 7/6          |              |
| FM 5   | total fraction            | 629           | —                                   | —                                   | 58.7                                 | 1114 | 101.3 | 86.01        | 7.284        |
| 2 FM 7 | +75 n. m.                 | 488           | —                                   | —                                   | 65.9                                 | 2248 | 210.5 | 83.23        | 9.480        |
| 2 FM 7 | 75-53 n. m.               | 578           | —                                   | —                                   | 71.7                                 | 2190 | 193.5 | 83.77        | 9.361        |
| 2 FM 7 | 75-53 n. m.               | 665           | —                                   | —                                   | 79.3                                 | 1334 | 119.5 | 84.04        | 9.303        |
| 2 FM 7 | 53-42 n. m.               | 638           | —                                   | —                                   | 74.9                                 | 2725 | 231.0 | 84.28        | 9.003        |
| 2 FM 7 | 53-42 n. m.               | 783           | —                                   | —                                   | 86.1                                 | 1688 | 141.4 | 84.43        | 9.197        |
| 2 FM 7 | —42 n. m.                 | 715           | —                                   | —                                   | 76.9                                 | 1396 | 120.9 | 85.06        | 8.419        |

## Val Colla zone

| Sample | Size fractions in microns | Atomic ratios | Apparent ages in my*)               |                                     |                                      |       |       | Atomic ratio | Apparent age |
|--------|---------------------------|---------------|-------------------------------------|-------------------------------------|--------------------------------------|-------|-------|--------------|--------------|
|        |                           |               | Pb <sup>206</sup> /U <sup>238</sup> | Pb <sup>207</sup> /U <sup>235</sup> | Pb <sup>207</sup> /Pb <sup>206</sup> | 6/8   | 7/5   | 7/6          |              |
| CHI 1  | +42 n. m.                 | 1582          | 279                                 | 50.7                                | 260.5                                | 29.50 | 29.50 | 90.39        | 4.31         |
| CHI 1  | +53 n. m.                 | 4660          | 1280                                | 113.3                               | 105.4                                | 20.43 | 20.43 | 83.75        | 11.31        |
| CHI 1  | —42 m.                    | 6370          | 1322                                | 136.6                               | 89.95                                | 19.29 | 19.29 | 85.18        | 9.42         |

\*) MAL 1 is identical with sample 1, and MAL 2 is identical with sample 2 in Pidgeon et al. (1970).

Table 3. Atomic ratios and apparent ages of zircons and monazite

| Sample             | Size fractions<br>in microns | Atomic ratios                       |                                     |                                      | Apparent ages in my*) |     |      | Atomic<br>ratio | Apparent<br>age |
|--------------------|------------------------------|-------------------------------------|-------------------------------------|--------------------------------------|-----------------------|-----|------|-----------------|-----------------|
|                    |                              | Pb <sup>206</sup> /U <sup>238</sup> | Pb <sup>207</sup> /U <sup>235</sup> | Pb <sup>207</sup> /Pb <sup>206</sup> | 6/8                   | 7/5 | 7/6  |                 |                 |
| Strona-Ceneri zone |                              |                                     |                                     |                                      |                       |     |      |                 |                 |
| <i>Group A</i>     |                              |                                     |                                     |                                      |                       |     |      |                 |                 |
| MAL 1              | 150-75                       | 0.07077                             | 0.5715                              | 0.05857                              | 445                   | 465 | 564  | —               | —               |
| MAL 1              | 75-53                        | 0.06893                             | 0.5394                              | 0.05675                              | 434                   | 444 | 494  | —               | —               |
| MAL 1              | 53-42                        | 0.06880                             | 0.5369                              | 0.05660                              | 433                   | 442 | 488  | —               | —               |
| MAL 1              | -42                          | 0.06882                             | 0.5357                              | 0.05645                              | 433                   | 441 | 482  | —               | —               |
| FM 17              | total fraction               | 0.07057                             | 0.5583                              | 0.05739                              | 444                   | 456 | 518  | —               | —               |
| FM 7               | total fraction               | 0.07747                             | 0.6150                              | 0.05757                              | 486                   | 493 | 526  | —               | —               |
| FM 12              | total fraction               | 0.07226                             | 0.5602                              | 0.05622                              | 454                   | 457 | 473  | —               | —               |
| <i>Group B</i>     |                              |                                     |                                     |                                      |                       |     |      |                 |                 |
| MAL 2              | 150-75 n. m.                 | 0.1297                              | 1.540                               | 0.08607                              | 794                   | 959 | 1362 | —               | —               |
| MAL 2              | 150-75 n. m.                 | 0.1283                              | 1.532                               | 0.08654                              | 786                   | 956 | 1374 | —               | —               |
| MAL 2              | 75-53 n. m.                  | 0.1271                              | 1.490                               | 0.08505                              | 778                   | 938 | 1340 | —               | —               |
| MAL 2              | 53-42 n. m.                  | 0.1220                              | 1.404                               | 0.08346                              | 749                   | 902 | 1302 | —               | —               |
| MAL 2              | -42 n. m.                    | 0.1154                              | 1.289                               | 0.08102                              | 711                   | 852 | 1244 | —               | —               |

| Sample         | Size fractions<br>in microns | Atomic ratios                       |                                     |                                      | Apparent ages in my <sup>*)</sup> |      |      | Atomic<br>ratio | Apparent<br>age |
|----------------|------------------------------|-------------------------------------|-------------------------------------|--------------------------------------|-----------------------------------|------|------|-----------------|-----------------|
|                |                              | Pb <sup>206</sup> /U <sup>238</sup> | Pb <sup>207</sup> /U <sup>235</sup> | Pb <sup>207</sup> /Pb <sup>206</sup> | 6/8                               | 7/5  | 7/6  |                 |                 |
| MAL 2          | 150-75 m.                    | 0.1137                              | 1.248                               | 0.07973                              | 701                               | 834  | 1212 | —               | —               |
| MAL 2          | 53-42 m.                     | 0.1150                              | 1.247                               | 0.07867                              | 708                               | 833  | 1184 | —               | —               |
| MAL 2          | -42 m.                       | 0.1092                              | 1.157                               | 0.07689                              | 674                               | 791  | 1138 | —               | —               |
| CEN 1          | +75 n. m.                    | 0.1488                              | 2.314                               | 0.1129                               | 903                               | 1232 | 1876 | —               | —               |
| CEN 1          | 75-53 n. m.                  | 0.1274                              | 1.734                               | 0.09885                              | 780                               | 1035 | 1629 | —               | —               |
| CEN 1          | 53-42 n. m.                  | 0.1148                              | 1.448                               | 0.09157                              | 707                               | 921  | 1483 | —               | —               |
| CEN 1          | 53-42 m.                     | 0.1129                              | 1.398                               | 0.08991                              | 696                               | 900  | 1448 | —               | —               |
| CEN 1          | -42                          | 0.1043                              | 1.194                               | 0.08313                              | 646                               | 808  | 1295 | —               | —               |
| CAS 1          | +75 n. m.                    | 0.1111                              | 1.227                               | 0.08023                              | 685                               | 824  | 1224 | 0.03688         | 742             |
| CAS 1          | 75-53 n. m.                  | 0.1033                              | 1.033                               | 0.07224                              | 640                               | 727  | 1012 | 0.03467         | 698             |
| CAS 1          | 53-42 n. m.                  | 0.09401                             | 0.8994                              | 0.06948                              | 586                               | 660  | 931  | 0.03202         | 646             |
| CAS 1          | -42                          | 0.09060                             | 0.8335                              | 0.06682                              | 564                               | 624  | 849  | 0.03243         | 654             |
| CAS 1 Monazite | total fraction               | 0.07027                             | 0.5393                              | 0.05580                              | 442                               | 444  | 456  | 0.02077         | 421             |
| CAS 1 Monazite | +75                          | 0.07191                             | 0.5601                              | 0.05647                              | 452                               | 458  | 481  | 0.02202         | 446             |
| CAS 1 Monazite | -42                          | 0.07275                             | 0.5618                              | 0.05600                              | 457                               | 459  | 464  | 0.02229         | 452             |
| 2 FM 5         | +75 n. m.                    | 0.1228                              | 1.612                               | 0.09522                              | 755                               | 988  | 1558 | —               | —               |
| 2 FM 5         | 75-53 n. m.                  | 0.1041                              | 1.184                               | 0.08257                              | 645                               | 804  | 1281 | —               | —               |
| 2 FM 5         | 53-42 n. m.                  | 0.09088                             | 0.9542                              | 0.07625                              | 566                               | 689  | 1122 | —               | —               |
| 2 FM 5         | -42                          | 0.08743                             | 0.8775                              | 0.07289                              | 545                               | 648  | 1029 | —               | —               |
| FM 5           | total fraction               | 0.09349                             | 1.011                               | 0.07844                              | 582                               | 719  | 1178 | —               | —               |
| 2 FM 7         | +75 n. m.                    | 0.1304                              | 1.572                               | 0.08753                              | 798                               | 972  | 1396 | —               | —               |
| 2 FM 7         | 75-53 n. m.                  | 0.1208                              | 1.365                               | 0.08203                              | 742                               | 885  | 1268 | —               | —               |
| 2 FM 7         | 75-53 m.                     | 0.1163                              | 1.269                               | 0.07922                              | 716                               | 843  | 1199 | —               | —               |
| 2 FM 7         | 53-42 n. m.                  | 0.1150                              | 1.262                               | 0.07968                              | 708                               | 839  | 1211 | —               | —               |
| 2 FM 7         | 53-42 m.                     | 0.1079                              | 1.122                               | 0.07553                              | 667                               | 774  | 1103 | —               | —               |
| 2 FM 7         | -42 n. m.                    | 0.1065                              | 1.125                               | 0.07665                              | 659                               | 776  | 1132 | —               | —               |
| Val Colla zone |                              |                                     |                                     |                                      |                                   |      |      |                 |                 |
| CHI 1          | +42 n. m.                    | 0.0336                              | 0.268                               | 0.0582                               | 215                               | 245  | 550  | 0.00905         | 185             |
| CHI 1          | +53 m.                       | 0.0236                              | 0.192                               | 0.0590                               | 152                               | 180  | 580  | 0.01126         | 229             |
| CHI 1          | -42 m.                       | 0.0214                              | 0.165                               | 0.0558                               | 138                               | 157  | 460  | 0.01095         | 223             |

\*) Errors are indicated in fig. 2 and 3.

Common lead correction: Pb<sup>206</sup>/Pb<sup>204</sup>: 17.66  
Pb<sup>207</sup>/Pb<sup>204</sup>: 15.26  
Pb<sup>208</sup>/Pb<sup>204</sup>: 37.04

n. m.: fraction of lower magnetic susceptibility  
m. fraction of higher magnetic susceptibility

## 3. STRONA-CENERI ZONE: RESULTS

## 3.1.1. U-Pb age patterns of zircon and monazite

The results of the isotope dilution analyses and the apparent ages are listed in tables 2 and 3 and illustrated in U-Pb and Th/Pb evolution diagrams (figs. 2, 3, 4). According to the apparent ages, two zircon groups can be distinguished:

- *Group A* comprises zircon suites with U-Pb ages between 430 and 490 my (fig. 3), and
- *Group B* contains zircons with U-Pb ages between 560 and 1230 my (fig. 2).

The apparent ages of the group A zircons are all very similar and almost concordant, whereas the apparent ages of the group B zircons are highly discordant and define a wedge with the lower intersection with the concordia curve at 450 to 500 my and two upper intersections at 1600 my and 2500 my. The data points of each suite show a nearly linear array. Both groups differ in the uranium concentrations as seen from table 2.

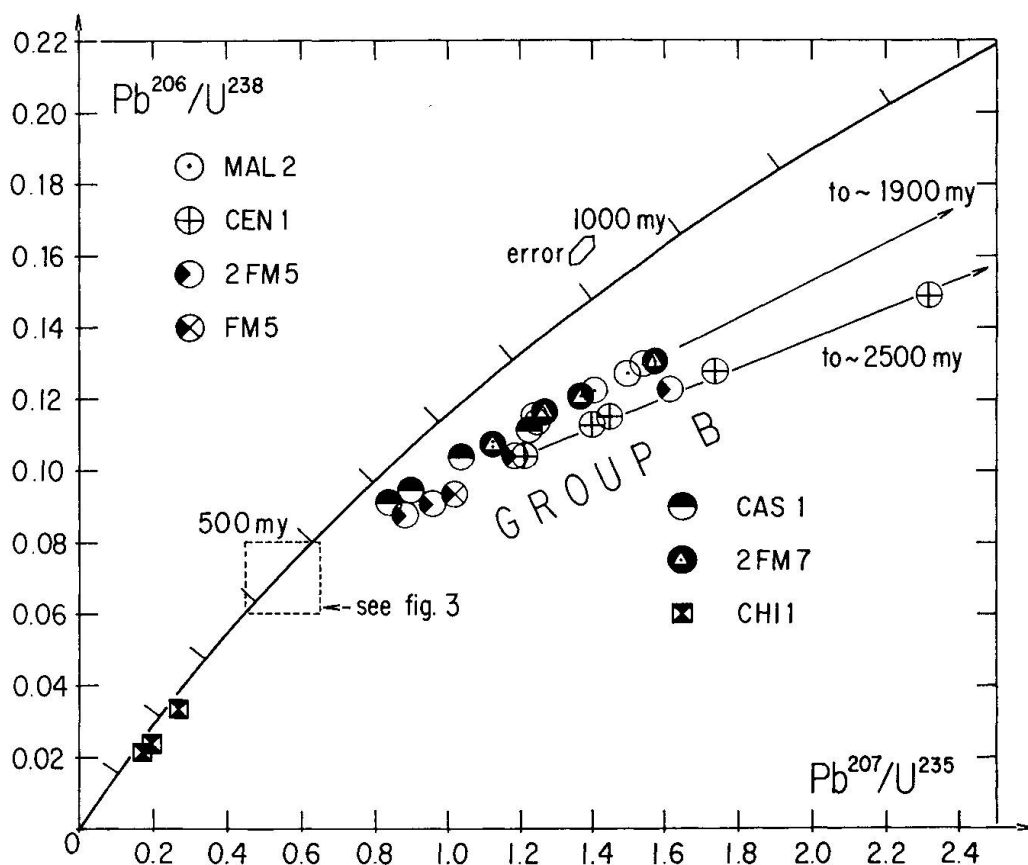


Fig. 2. U-Pb evolution diagram (concordia diagram) showing the data points of the group B paragneiss zircon suites from the Strona-Ceneri zone and of sample CHI 1 from an alkali-feldspar-gneiss (Chiari gneiss) of the Val Colla zone.

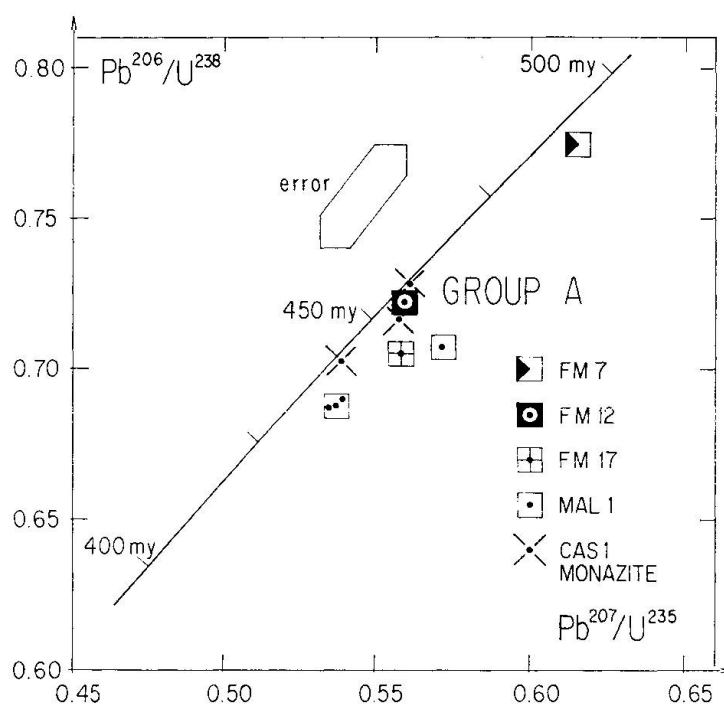


Fig. 3. U-Pb evolution diagram showing the data points of the group A zircons from granitic gneisses (MAL 1, FM 17), a transitional rock type (FM 7), and a paragneiss (FM 12) of the Strona-Ceneri zone. The monazite was separated from the paragneiss sample CAS 1, the zircons of which belong to group B (fig. 2).

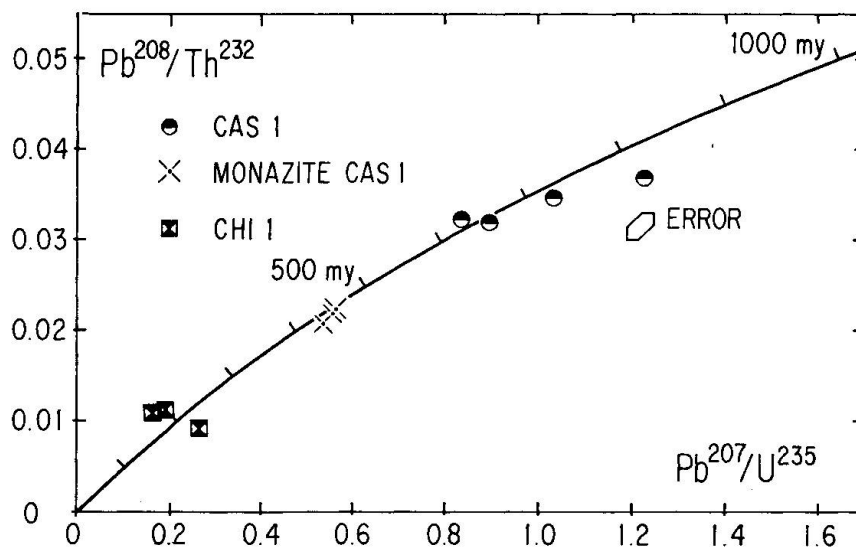


Fig. 4. U-Th-Pb evolution diagram showing the data points of the zircon and monazite fractions of the paragneiss sample CAS 1 from the Strona-Ceneri zone and of the zircon fractions of the aplitic alkali-feldspar-gneiss CHI (Chiari gneiss) of the Val Colla zone.

The ages of monazite from a paragneiss containing group B zircons are concordant at  $450 \pm 10$  my and are therefore similar to the apparent ages of the group A zircons.

Table 4. *The morphological properties of zircons observed under the microscope.*

|                           | Group A: almost concordant zircons of Caledonian age   | Group B: highly discordant zircons of pre-Caledonian age   |
|---------------------------|--|--|
| <i>Strona-Ceneri zone</i> |  |  |
| Rock type                 | <p><i>Granitic gneiss</i>: K-feldspar-biotite-plagioclase-gneiss: samples MAL 1, FM 17.</p> <p><i>Transitional rock type</i>: biotite-plagioclase-gneiss containing K-feldspar: sample FM 7.</p> <p><i>Paragneiss</i>: Al-rich gneiss with traces of K-feldspar: sample FM 12.</p> | <p><i>Paragneisses</i>:</p> <p>Hornfelsic biotite-plagioclase-gneiss: sample MAL 2.</p> <p>Granulated biotite-plagioclase-gneiss with lime silicate inclusions: samples CEN 1, CAS 1.</p> <p>Biotite-muscovite-plagioclase-gneiss: samples FM 5, 2 FM 5.</p> <p>Biotite-plagioclase-gneiss with lime silicate inclusions: sample 2 FM 7.</p> |
| Habit                     | Euhedral, prismatic, smooth crystal faces; principal crystal faces: (100), (110), (101), (111), (fig. 6); subordinate crystal faces: (311).  | Short prismatic, rounded, pitted crystal faces: samples MAL 2, 2 FM 7 (fig. 7); euhedral, prismatic, smooth crystal faces, principle crystal faces: (311), (100), (110), subordinate crystal faces: (101, (111): sample CAS 1 (fig. 7). Both zircon types are present in samples CEN 1, 2 FM 5, and FM 5.                                    |
| Zonal-growth              | Widespread (fig. 6).   | Rare in sample MAL 2, absent in the other samples.   |
| Color                     | Pink with a violet cast. Translucent domains in all suites, opaque domains are widespread.   | Pink with a violet cast, mainly transparent, no opaque domains.  |
| <i>Val Colla zone</i>     |  |  |
| Rock type                 | Muscovite-alkali-feldspar-gneiss: sample CHI 1.  |  |
| Habit                     | Identical to the group A zircons of the Strona-Ceneri zone.  |  |
| Color                     | Greyish with a green cast, widespread zonal growth, opaque domains and grains common.  |  |

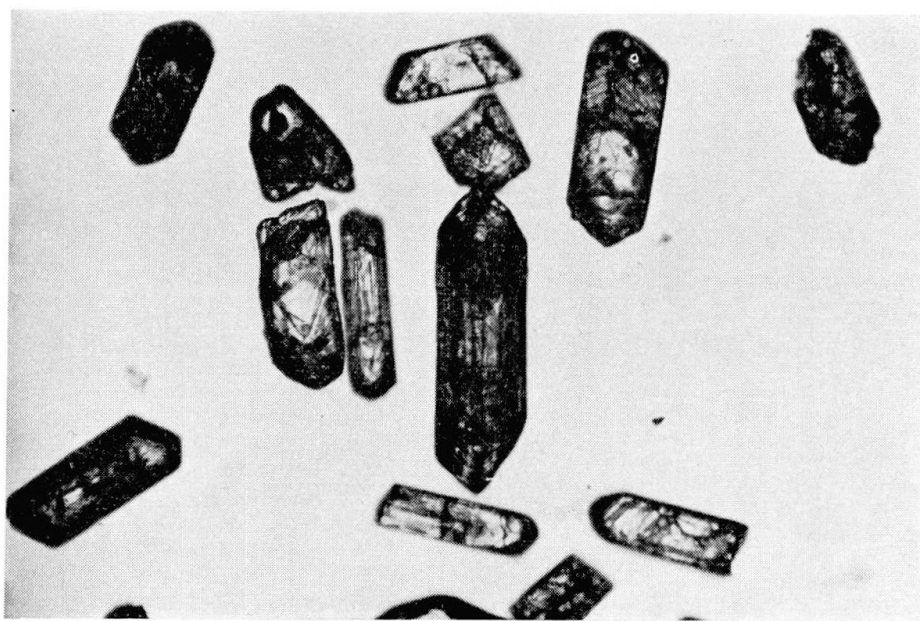


Fig. 5.  $200\times$ . Newly formed zircons of group A from sample MAL 1 showing zonal growth and the characteristic crystal habit.

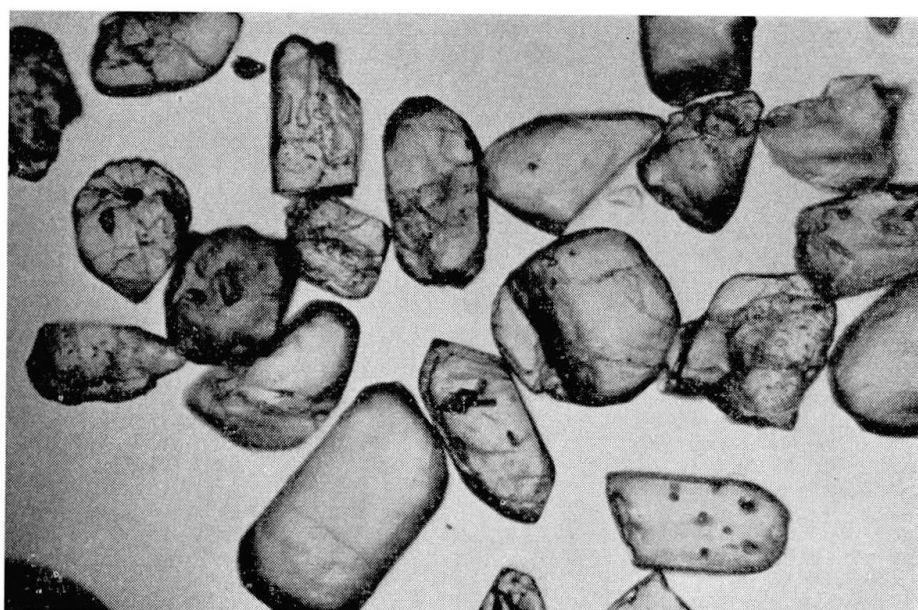


Fig. 6.  $500\times$ . Detrital zircons of group B from sample MAL 2.  
Few grains show enhydral, recrystallised faces.

### *3.1.2. Host rocks, morphology and colour*

In table 4 the morphology and the colour of the zircon populations observed under the microscope are listed for the respective host rocks. Whereas the host rocks of the group A zircons are granitic gneisses, transitional rocks and a neighbouring paragneiss, we find only paragneisses as host rocks of the group

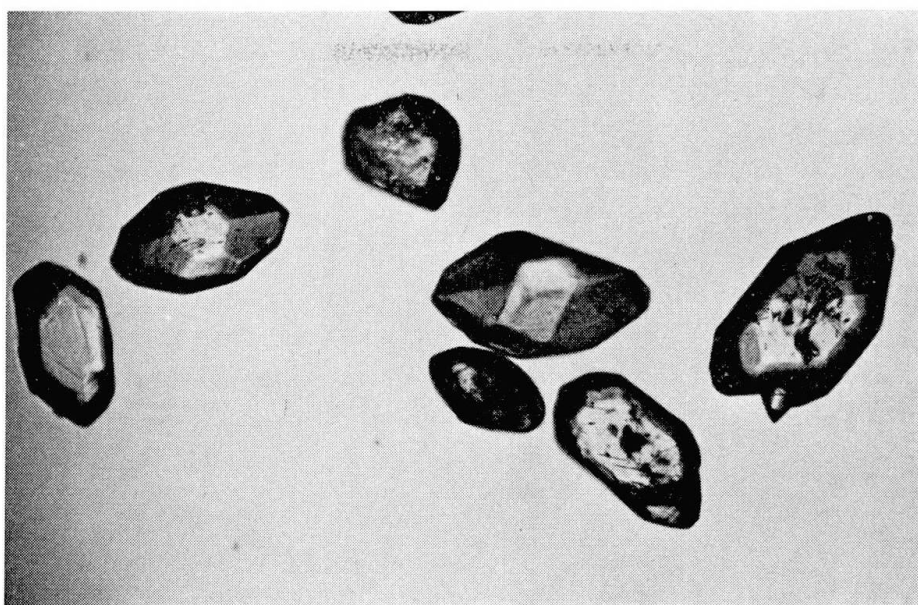


Fig. 7.  $500\times$ . Zircons of group B from the paragneiss sample CAS 1 showing the characteristic habit of the euhedral zircons of group B with dominant pyramids and subordinate prisms. Mineralogical evidence points to a recrystallisation of these zircons while retaining a similar amount of trace elements as the rounded zircons of group B which were annealed during the amphibolite facies metamorphism.

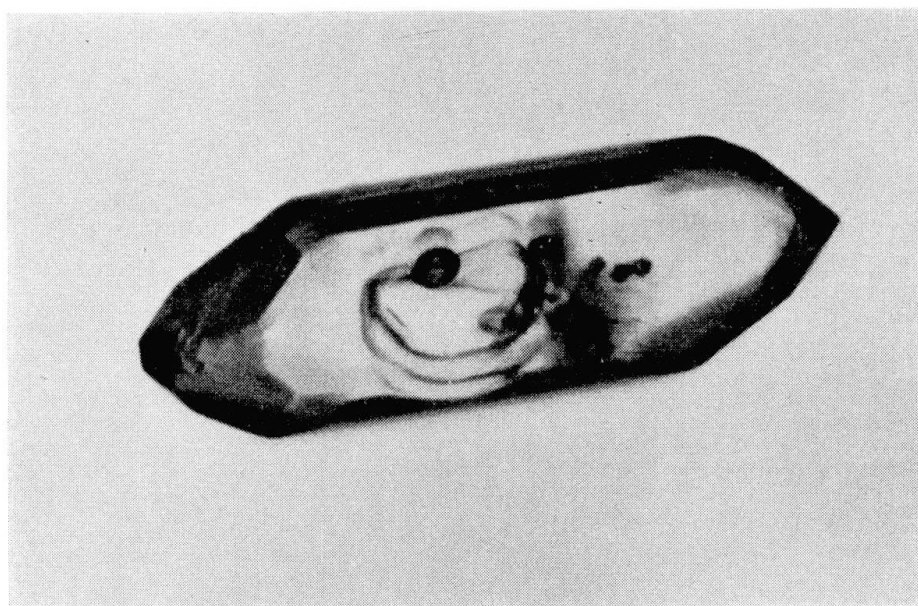


Fig. 8.  $600\times$ . Newly formed zircon of group A, sample MAL 1, with a rounded zircon core.

B zircons. The occurrence of zircons yielding almost concordant ages is therefore not solely restricted to granitic gneisses.

Table 4 reveals that the two zircon groups are distinguished by their crystal habit, the presence or absence of zonal growth, and their degree of transparency.

### 3.1.3. Electron microprobe investigation

Because of the different apparent ages and morphologies of the two zircon groups it was hoped that significant distinctions in the trace element content and distribution in the two zircon groups would yield further information concerning their history and genesis.

Of each suite 10 to 30 U-P, 10 Y-P, and 10 Ca-P profiles were recorded with an ARL electron microprobe. All concentrations were semiquantitatively calibrated. Hf appears to be present in similar concentrations in all zircons.

The averaged Y and P values of each zircon suite were normalised to the values of the suite with the lowest trace element content. Thus the values of the group B zircons for Y and P vary between 1 and 2.2 and 1 and 2.6 respectively.

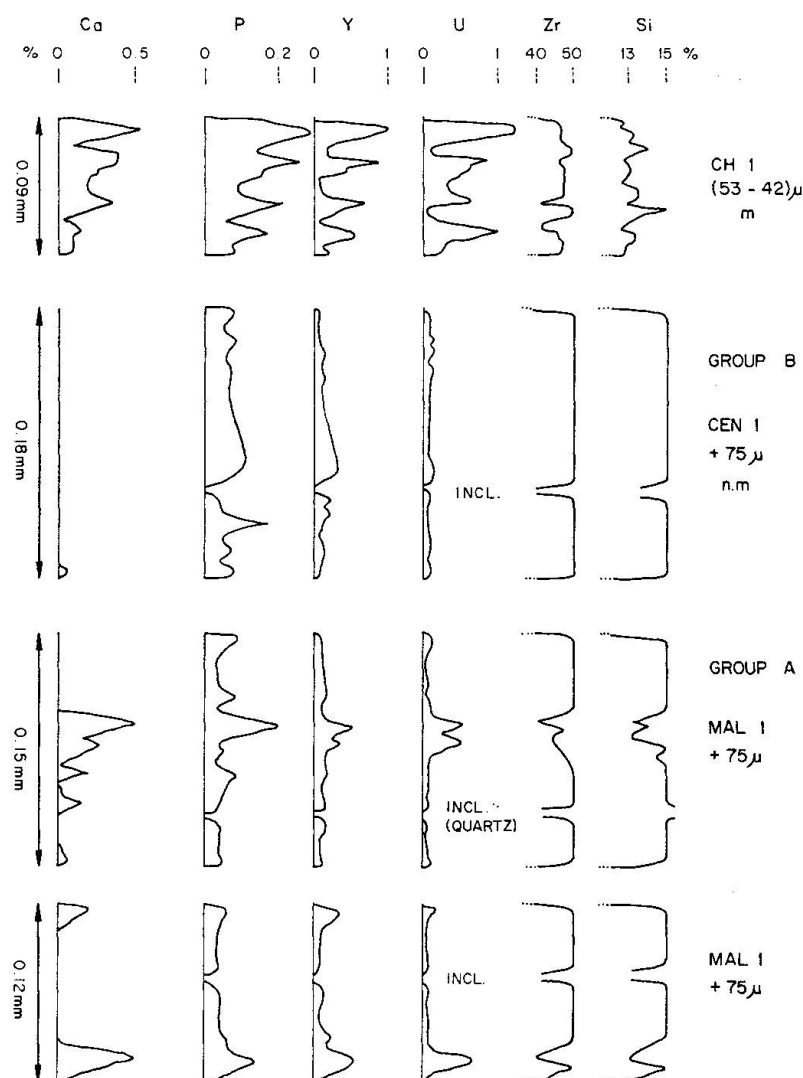


Fig. 9. Representative electron microprobe profiles of Si, Zr, U, Y, P, and Ca for group A and B zircons and for the fraction of higher magnetic susceptibility of sample CHI 1. The concentrations are semiquantitatively calibrated.

The corresponding values for the group A zircons are 2.1 to 4.4 and 2.0 to 2.6. Because of the occasional presence of apatite as inclusions in zircons, no relative Ca content has been calculated.

Fig. 9 shows the Si, Zr, U, Y, P, and Ca distributions across individual zircon grains. The distribution of the trace elements is in both zircon groups inhomogeneous. The major part of the observed area of each zircon grain contains several 100 to about 1000 ppm U and several 100 to a few 1000 ppm P and Y. The Ca content is generally below the detection limit; rarely does it reach a few 1000 ppm. In these areas no correlation of the trace element concentrations is visible.

In contrast, in areas of trace element concentrations of up to 10 000 ppm a positive correlation between the U, Ca, P, and Y contents is observed.

The group A zircons contain more domains with high trace element contents than those of group B. In addition there is a tendency of the group A zircons to have an outer crystal portion where the trace elements are enriched on the average by a factor of 1.3–1.5 as compared to the inner part.

The question remains open whether these elements form a separate phase in the zircons or whether they substitute for Zr and Si in the crystal lattice.

Table 5. *Cell dimensions*

| Sample                      | $a_0$ (Å)         | $c_0$ (Å)         |
|-----------------------------|-------------------|-------------------|
| Synthetic zircon            | $6.608 \pm 0.001$ | $5.982 \pm 0.001$ |
| Synthetic zircon            | $6.609 \pm 0.001$ | $5.983 \pm 0.001$ |
| <i>Strona-Ceneri zone</i>   |                   |                   |
| <i>Group A</i>              |                   |                   |
| MAL 1, +75 $\mu$            | $6.612 \pm 0.002$ | $5.998 \pm 0.004$ |
| FM 7                        | $6.611 \pm 0.001$ | $5.988 \pm 0.001$ |
| FM 12                       | $6.618 \pm 0.001$ | $5.997 \pm 0.002$ |
| <i>Group B</i>              |                   |                   |
| MAL 2, +75 $\mu$ , n. m.    | $6.607 \pm 0.001$ | $5.984 \pm 0.002$ |
| MAL 2, 53–75 $\mu$ , n. m.  | $6.614 \pm 0.002$ | $5.988 \pm 0.002$ |
| CEN 1, +75 $\mu$ , n. m.    | $6.609 \pm 0.001$ | $5.988 \pm 0.002$ |
| CAS 1, +75 $\mu$ , n. m.    | $6.607 \pm 0.001$ | $5.987 \pm 0.002$ |
| 2 FM 5, +75 $\mu$ , n. m.   | $6.610 \pm 0.001$ | $5.989 \pm 0.001$ |
| 2 FM 5, 42–53 $\mu$ , n. m. | $6.610 \pm 0.002$ | $5.991 \pm 0.002$ |
| 2 FM 5, 42–53 $\mu$ , m.    | $6.609 \pm 0.001$ | $5.990 \pm 0.001$ |
| 2 FM 7, +75 $\mu$ , n. m.   | $6.611 \pm 0.001$ | $5.988 \pm 0.001$ |
| <i>Val Colla zone</i>       |                   |                   |
| CHI 1, 42–53 $\mu$ , m.     | $6.616 \pm 0.002$ | $5.999 \pm 0.004$ |
|                             | $6.643 \pm 0.001$ | $6.025 \pm 0.002$ |

The X-ray powder diffraction patterns were recorded with the aid of a Jagodzinski camera using Fe radiation. The sample and the film were held under vacuum. 1 sigma errors are stated.

### 3.1.4. Cell dimensions

In table 5 the cell dimensions are listed. These have been calculated from 9 to 14 reflections using a least square program for the refinement. Slightly higher values for  $c_0$  are observed in the zircons of group A as compared to the group B.

In the range of an uranium concentration averaging 400 to 800 ppm, there is no noticeable correlation between the cell dimensions and the uranium content (see samples 2 FM 5 and MAL 2).

The X-ray powder diffraction patterns of the group A zircons are more diffuse than those of the group B zircons.

## 3.2. Discussion

### 3.2.1. Group A zircon and monazite data

PIDGEON et al. (1970) concluded from the almost concordant ages of sample MAL 1 that 420–440 my ago the rocks were affected by a severe metamorphism that led to a complete reconstitution of the zircons in the granitic gneiss. These conclusions are supported by the ages of sample FM 17 (444–518 my) of the same type of granitic gneiss from a different locality.

Independent evidence for a Caledonian event is gained from the concordant ages of monazite fractions of the paragneiss sample CAS 1. These ages place the event during the Caledonian orogeny at  $450 \pm 10$  my. Other evidence for the existence of a Caledonian event within the Alps are the Rb-Sr isochron and zircon ages from the Silvretta nappe and the Gotthard massif (GRAUERT 1966, GRAUERT and ARNOLD, 1968, GRAUERT, 1969, ARNOLD, 1970).

The zircon ages (486–526 my) of the transitional rock type FM 7 and from the paragneiss sample FM 12 (454–473 my) demonstrate that the reconstitution of the zircons was not restricted to the granitic gneiss alone. This process took place in the transitional rock type, that was sampled approximately 100 m from an aplitic alkali-feldspar-gneiss, as well as in a paragneiss about 100 m away from a zone of transitional rock type. Characteristic of the occurrence of group A zircons is the presence of K-feldspars in the host rocks.

The euhedral habit and the absence of microscopically visible cores of an older zircon generation in the majority of the crystals suggest that the zircons were newly formed during the metamorphism of the rock (fig. 5). Further evidence for a new zircon growth is the abundance of domains rich in trace elements. The domains are located in the interior as well as in the outer portion of the crystals (fig. 9). The group A zircons therefore do not represent a pre-metamorphic zircon generation, comparable to the group B zircons, that gained a new outer shell rich in trace elements during the granitisation process.

The somewhat larger cell dimensions of the group A zircons is considered to be the result of their higher trace element content. The X-ray powder patterns of the group A zircons are more diffuse than those of the B group, indicating thereby that the lattice of the group A zircons is more disturbed due to a domain structure. Such a domain structure also suggests that the zircons were newly formed and not recrystallised.

The high apparent ages of the coarsest grain size fraction of sample MAL 1 (fig. 3) cannot be the result of an inadequate common lead correction. The composition of a common lead yielding in this case concordant ages of 440 my would be unusually high in  $\text{Pb}^{207}$  compared to  $\text{Pb}^{206}$  ( $\text{Pb}^{207}/\text{Pb}^{204} = 19.91$ ,  $\text{Pb}^{206}/\text{Pb}^{204} = 21.09$ ). PIDGEON et al. (1970) interpreted the high apparent ages as being due to a small quantity of inherited older radiogenic lead (approximately 1%), which might be located in the occasionally visible rounded zircon cores occurring as inclusions in euhedral zircon crystals (fig. 8).

The high apparent ages of sample FM 7 may be explained in the same manner. More complex explanations would involve either two periods of zircon growth, following closely on each other, in different areas of the Southern Alps, or else a higher age for the metamorphism and period of zircon formation, and a subsequent (Hercynian?) lead loss. This latter interpretation implies that monazite and zircon as well as their U-Pb systems respond differently to given p-t conditions.

### 3.2.2. Group B zircon data

PIDGEON et al. (1970) considered the paragneiss zircons as a detrital and therefore most probably heterogeneous mixture of different populations having different primary ages; furthermore the U-Pb systems of these populations were most likely disturbed prior to the mixing process. The linear array of the data points of sample MAL 2 was explained as a combined effect of averaging a mixed suite by sizing and a drastic lead loss during the Caledonian metamorphism. The intersections of the best fit line through the sample points of such a mixture with the concordia curve has no geological significance. The upper intersection with the concordia curve of a line drawn through the time mark of the episodic loss and through the data point with the lowest  $\frac{\text{Pb}^{206}/\text{U}^{238}}{\text{Pb}^{207}/\text{U}^{235}}$  ratio gives a minimum age of the oldest population present in the suite.

The small possible range for lower intersections of the best fit lines through the sample points of the group B zircon suites can only be explained if either all zircon populations of the mixture had approximately equal apparent or true ages, or else the populations with widely different primary ages were well mixed during the sedimentation process.

It is noteworthy that the sample points of the coarsest grain size fraction of all suites, except one, lie below the best fit line through the sample points

of the finer fractions. The coarsest grain size fractions contain therefore either a higher proportion of older zircons than the finer fractions, or else the coarse-grained crystals contain in their cores an older radiogenic lead component that was incorporated at the time of their formation as was the case in the coarsest grain size fraction of sample MAL 1 from the group A zircons.

PIDGEON et al. (1970) thought the amphibolite facies metamorphism to be the principal cause for the lead loss of the paragneiss zircons. Grauert (personal communication), however, obtained similarly discordant zircon ages from greenschist facies phyllites within the Silvretta nappe. MICHOT and DEUTSCH (1969) also report highly discordant zircon ages with equally low uranium contents from greenschist facies sediments in Brittany. The degree of discordancy is therefore not directly related to the degree of metamorphism.

Uranium gain, as an alternative explanation for the discordant ages, appears unlikely in view of the uranium distribution pattern within the crystals (fig. 9). On the contrary, during the sedimentation process the paragneiss zircons may have lost through mechanical abrasion the uranium-rich outer rims which seem to be typical of newly formed zircons.

There remains the possibility of uranium gain through new zircon growth (SAXENA, 1966) during diagenesis and metamorphism. Based on morphological criteria this possibility can be of only minor importance in those suites which contain besides rounded zircons some botryoidal intergrowths of several small crystals that may not be of detrital origin.

Samples CAS 1, in part also CEN 1 and 2 FM 5, contain zircons showing a morphology which suggests that they never underwent a process of abrasion (fig. 7). The two zircon types, rounded and euhedral, of group B cannot be distinguished either with respect to their U, Y, P, and Ca distribution patterns or in their content of these elements. Also, the apparent ages of the suite CAS 1, which are the same as those of the other paragneiss suites, rules out the possibility that the euhedral paragneiss zircons were newly formed during the metamorphism.

STERN et al. (1966) have shown an example of a drastic lead loss in zircons due to weathering. Such a disturbance of the U-Pb systems of the paragneiss zircons may account for the discrepancy between the concordant monazite ages and the time mark of the lower intercept of the zircon arrays.

On a Th-U-Pb diagram (fig. 4) the data points of sample CAS 1 do not form a linear array. They indicate that in addition to an unfractionated lead loss either a Th loss or U gain took place during the metamorphism. A preferential loss of U-lead may be envisaged if the zircons consist of two or more phases with varying U/Th ratios which loose lead at different rates (STEIGER and WASSERBURG, 1966).

The lattice constants of the group B zircons are (table 5) closer to the lattice constants of pure synthetic zircons than are those of the group A zir-

cons, and hence reflect their low trace element content. Furthermore, the X-ray diffraction patterns of the group B zircons are less diffuse than of group A. According to their greater age and higher radiation dosage of the group B zircons one would expect them to show a higher degree of radiation damage than the group A zircons. If the degree of lattice disturbance, as shown by the diffusiveness of the X-ray powder diffraction patterns, is only related to the radiation damage, then the observed relatively low degree of lattice disturbance of the group B zircons points to an annealing process that most likely took place during the metamorphism. In the paragneiss samples CAS 1, CEN 1, 2 FM 5, and FM 5 the annealing process was coupled with recrystallisation leading to the formation of euhedral crystals. The recrystallised, euhedral zircons retained a similar amount a trace elements as those that were only annealed.

Whether the low trace element content of the group B zircons is a consequence of the annealing process or not cannot be decided. It could well be that only nearly perfect zircons, i. e. zircons poor in trace elements, survive any prolonged weathering and sedimentation process (CARROLL, 1953, RAESIDE, 1959).

In the foregoing discussion it was assumed that the paragneisses of the Southern Alps represent the metamorphosed sedimentary filling of a Caledonian geosyncline. An alternative hypothesis compatible with the zircon ages would regard the Southern Alps as part of an approximately 2000 my old shield area that underwent Caledonian metamorphism leading to the formation of granitic gneisses. The only argument against this hypothesis are GRAUERT'S (1969) conclusions with regard to the sedimentation age of the paragneisses of the Silvretta nappe. Based on Rb-Sr data he derived a sedimentation age of  $510 \pm 60$ . If the geological evidence pointing to the Southern Alps as the most probable hinterland of the crystalline core of the Silvretta nappe is correct (TERMIER, 1905, STAUB, 1950), then the Southern Alps were initiated during the Caledonian orogeny.

#### 4. VAL COLLA ZONE: RESULTS AND DISCUSSION, SAMPLE CHI 1

The results are listed in tables 2, 3, 4, and 5 and the data points are plotted on a concordia diagram in fig. 2 and 4. The morphology of the zircons is identical to that of the group A zircons from the Strona-Ceneri zone. The uranium concentration (1580 ppm) of the fraction of lower magnetic susceptibility is similar to that of the group A zircons (1000–1600 ppm), and contrasts with the high uranium concentrations of the fractions of high magnetic susceptibility (4600–6400 ppm). The P, Y, and Ca contents are in both fractions higher than in the group A zircons. The distribution pattern of the trace

elements is similar to those of the group A zircons, except that crystals rich in trace elements contain several zones, starting in the center, in which these elements are enriched (fig. 9).

The X-ray powder diffraction pattern is even more diffuse than the ones of the group A zircons. All reflections with a  $2\theta$  value of  $41^\circ$  (211 reflection) and higher are doubled showing that the zircons consist of two phases. It is assumed that the phase with the smaller lattice constants, which are similar to the group A zircons, corresponds to the zircon phase with relatively low trace element contents as observed in the fraction of lower magnetic susceptibility, and conversely that the phase with the larger cell dimensions corresponds to the phase with a relatively high trace element content.

Evidence that zircons are multiphase assemblages with respect to the U-Pb system has already been presented by GRÜNENFELDER (1963). The author observed a correlation between the degree of discordancy of the U-Pb ages on one hand and the water and trace element concentrations, the degree of transparency, and the presence or absence of a domain structure on the other hand. STEIGER and WASSERBURG (1966) concluded from the U-Th-Pb age patterns that the zircons represent a multiphase system and the findings of the microprobe investigation supported their view. KÖPPEL (1968) reported the existence of two zircon phases with different U and Ca contents and varying physical properties within a single zircon crystal, which, in addition, contained uraninite and a U-Th-silicate as inclusions.

The above mentioned properties of the zircon population of sample CHI 1 exclude the possibility that the analysed sample of Chiari gneiss represents a metamorphosed arkose. It appears most likely that the rock was formed during a granitisation process or else that it represents a differentiate of anatectic origin.

The highly discordant apparent ages cannot be readily explained by an episodic lead loss. According to field evidence the last major tectonic activity occurred between the Westphalian and the Permian (REINHARD, 1953) and therefore predates the apparent U-Pb ages. On the other hand, the Alpine orogeny only gently folded the Southern Alps as observed in the sedimentary cover.

Geological evidence shows that the Val Colla and the southeastern part of the Strona-Ceneri zone were situated since the Permian time close to the surface; therefore, a lead loss due to weathering should have affected all zircons and should also be visible in the group A zircons. The pronounced pre-Permian cataclasis of the rocks of the Val Colla zone may have facilitated the circulation of ground water that leached lead out of the zircons. Microscopic examination of thin sections reveals, however, no signs of a more drastic alteration than that found in the rocks of the Strona-Ceneri zone.

If one assumes a continuous lead loss then the question arises why sample

MAL 1 from the Strona-Ceneri zone with an uranium concentration and distribution similar to that of the fraction of lower magnetic susceptibility of sample CHI 1 has not also lost lead continuously. Aside from the higher Y, P, and Ca contents of sample CHI 1, which in itself may be the cause of a different behaviour of the U-Pb systems, there remains the possibility that the uranium of sample CHI 1 is incorporated differently to the uranium of sample MAL 1. In one case it may form together with Y, P, and Ca a separate phosphate phase, whereas in the other case the uranium is held in solid solution in the zircon lattice.

The Th-Pb ages demonstrate that the Th-Pb system did not behave in the same way as the U-Pb system (fig. 4). It is noteworthy that the fraction with the lowest Th and U contents yielded the lowest Th-Pb age but the highest U-Pb ages; the apparent ages may be explained by unfractionated lead loss. In contrast, the samples with high Th and U contents yielded high Th-Pb but low U-Pb ages, indicating either a Th loss or a U gain or else a preferential loss of  $Pb^{207}$  and  $Pb^{206}$  from different phases with distinct U/Th ratios (STEIGER and WASSERBURG, 1966).

The question remains open whether the Chiari gneiss is of Hercynian or Caledonian origin. The lead-lead ages point to an even greater age. However, the uncertainty of the large common lead correction introduces a considerable error in the lead-lead age, and furthermore it has been shown that newly formed zircons may contain an older radiogenic lead component that raises their lead-lead ages above the true age. An early Hercynian age as a lower limit is indicated by the occurrence of Chiari gneiss components in the West-phalian conglomerates (GRAETER, 1951, REINHARD, 1964).

## 5. SUMMARY

### 5.1. Zircons

The zircons of the Strona-Ceneri zone are divided according to the apparent ages into two groups. Group A comprises zircons with almost concordant Caledonian ages, whereas the group B zircons yielded highly discordant, pre-Caledonian ages.

The group A zircons are euhedral, exhibit zonal growth, are translucent to transparent, have a higher trace element concentration than the group B zircons, and show a domain structure. The group A zircons occur in granitic gneisses (believed to represent granitised sediments), in partially granitised (metasomatised) gneisses (transitional rock type), and in neighbouring paragneisses as far as 100 m away. All evidence points to a new formation of zircons closely related to the granitisation process.

A correlation appears to exist between the zircon formation process and the presence of K-feldspar in the rock: rocks containing K-feldspar, even in amounts of less than 1%, contain newly formed zircons, whereas rocks virtually free of K-feldspar contain detrital zircons yielding highly discordant apparent ages.

As group A zircons were never found to occur together with zircons of the group B, either only rocks very poor in zircons were granitised, or else the existing zircons were almost completely dissolved during the anatexis. The latter hypothesis is favoured because of the presence of small amounts of an older radiogenic lead component in the coarsest grain size fraction of the group A zircons. The presence of such an older lead component is considered to be indicative of an incomplete dissolution of pre-existing zircons.

The effect of the granitisation process coupled with a regional metamorphism on the zircons differs notably from the observations made by DAVIS *et al.* (1968) on zircons from the contact metamorphic aureole of the Eldora granite where the zircons retained high lead-lead ages as near as 0.5 m away from the contact and where the U-Pb ages start to decrease only 10–20 m away from the contact.

The zircons from the K-feldspar-free paragneisses define the group B. The zircons have all similarly low U, P, Y, and Ca contents. The distribution of these elements is more homogeneous than in the group A zircons. Two types of group B zircons occur, either separately in different paragneiss samples or together in the same sample. One type is rounded with pitted crystal faces, the other type is euhedral with smooth crystal faces but with a crystal habit distinctly different from that of the group A zircons. The group B zircons are more transparent than the group A zircons. Domain structure of the crystal lattice is less pronounced. All observations suggest that the group B zircons were annealed during the amphibolite facies metamorphism and that in places they have recrystallised.

The generally low trace element content of the group B zircons is considered to be the result of a combined effect of

- a mechanical abrasion of an outer crystal portion rich in trace elements,
- a lower resistibility of zircons rich in trace elements to weathering and sedimentation processes, and
- a loss of trace elements during the annealing and recrystallisation of the zircons.

In addition, the high discordancy may be partly due to a small uranium gain through new zircon growth during the metamorphism.

Different behaviour of the U-Pb systems of zircons is demonstrated by the concordant ages of sample MAL 1 and the highly discordant ages of sample

CHI 1. It is believed that the behaviour is governed by the trace element concentrations and also by their manner of incorporation in the zircon crystals. The zircons of sample CHI 1 consist, according to their X-ray powder diffraction pattern, of two phases with differing trace element concentrations.

### 5.2. Monazite

The concordant monazite ages demonstrate the usefulness of this mineral for dating purposes specifically in metamorphic terrains. Later thermal events as recorded by the K-Ar ages of the region did not have any effect on the U-Th-Pb system of the monazite.

### 5.3. Geochronology of the central part of the Southern Alps

The amphibolite facies metamorphism is dated according to the concordant monazite ages and the almost concordant zircon ages from the granitic gneisses and the adjoining rocks at  $450 \pm 10$  my. The paragneisses represent the sedimentary filling of a Caledonian geosyncline containing detritus from ancient shield areas some of which at least 2500 my old. Where these source regions were situated is still unknown.

In accordance with petrographic evidence the age pattern of the zircons from the granitic gneisses point to a sedimentary origin of the material.

The K-Ar age cluster of around 320 my (McDOWELL, 1970) may reflect a rapid cooling in upper Carboniferous time towards the end of an uplift of the basement. In the western part of the Strona-Ceneri zone this uplift would then have occurred later, i. e. 180–200 my ago.

Alternatively the clusters of K-Ar ages may reflect events unrelated to each other, i. e. separate periods of reheating and cooling.

The age of the Chiari gneiss remains unknown. Nevertheless one may reasonably assume that the rock was formed during the Caledonian orogeny or during an early Hercynian phase of magmatic and metamorphic activity.

### *Acknowledgements*

We wish to thank B. Grauert, P. Nunes, P. Signer and R. H. Steiger for helpful discussion of the paper, J. Sommerauer for his assistance in the electron microprobe work, and J. Felsche, E. Hilti, H. Schulz and V. Tscherry for their help in the X-ray work.

## APPENDIX

## Sample location

- MAL 1: from an abandoned quarry between Pura and Curio (coordinates: 710.20/94.85) <sup>4)</sup> <sup>5)</sup>.
- FM 7: from a cut along the road Vira-Indemini (coordinates: 780.10/109.70) <sup>1)</sup> \*).
- FM 12: north of Tesserete in the Val Capriasca (coordinates: 718.25/105.81) <sup>3)</sup> \*).
- MAL 2: from a road cut between Aranno and Forcora (coordinates: 711.60/97.20) <sup>4)</sup> <sup>5)</sup>.
- CEN 1: from an abandoned quarry between Magadino and Quartino (coordinates: 711.56/111.93) <sup>1)</sup>.
- CAS 1: from a road cut at Ponte Casletto, Val Grande (coordinates: 680.93/93.97) <sup>2)</sup>.
- 2 FM 5: same sample location as CEN 1.
- FM 5: same sample location as CEN 1.
- 2 FM 7: from a cut along the road Vira-Indemini (coordinates: 708.16/109.59) <sup>1)</sup>.
- FM 17: south of Astano (coordinates: 706.90/96.00) <sup>4)</sup> \*).
- CHI 1: east of Taverne (coordinates: 715.73/102.26) <sup>3)</sup>.

\*) Sample collected by McDowell.

The coordinates refer to those of the Swiss Federal Topographic Survey. Detailed petrographic descriptions are found in:

- <sup>1)</sup> BÄCHLIN, 1937.  
<sup>2)</sup> BORIANI, 1968.  
<sup>3)</sup> REINHARD, 1964.  
<sup>4)</sup> GRAETER, 1951.  
<sup>5)</sup> PIDGEON et al., 1970.

## REFERENCES

SMPM = Schweiz. Mineralogische und Petrographische Mitteilungen

- ARNOLD, A. (1970): On the history of the Gotthard massive (central Alps, Switzerland). *Eclogae. geol. Helv.* 63, 29–30.
- BÄCHLIN, R. (1937): Geologie und Petrographie des M. Tamaro-Gebietes. SMPM 17, 1–78.
- BORIANI, A. (1968): Il settore meridionale del gruppo del Monte Zeda (Lago Maggiore, Italia): Osservazione petrogenetiche. SMPM 48/1, 175–188.
- (1970a): The microstructure of “Cenerigneisses”. *Rend. Soc. Ital. Mineral. Petrologia*, 26/2, 487–501.
- BORIANI, A., RISARI, E. C. (1970b): The xenoliths of “Cenerigneisses”. *Rend. Soc. Ital. Min. Petrologia*, 26/2, 503–515.
- BORIANI, A. (1970c): The “Pogallo” line and its connection with the metamorphic and the anatectic phases of “Massiccio dei Laghi” between Ossola Valley and Lake Maggiore (Northern Italy). *Boll. Soc. Geol. Ital.*, 89, 415–433.
- CARROLL, D. (1953): Weatherability of zircon. *J. Sed. Petrology*, 23, 106–116.
- DAVIS, G. L., HART, S. R., TILTON, G. R. (1968): Some effects of contact metamorphism on zircon ages. *E.P.S.L.*, 5, 27–34.
- EL TAHLAWI, M. R. (1965): Geologie und Petrographie des nordöstlichen Comerseegebietes (Provinz Como, Italien). *Mitt. Geol. Inst. ETH u. Universität Zürich*, N.F. 27.
- GRAETER, P. (1951): Geologie und Petrographie des Malcantone (südliches Tessin). SMPM 31/2, 361–483.

- GRAUERT, B. (1966): Rb-Sr age determinations on orthogneisses of the Silvretta (Switzerland). *E.P.S.L.*, 1, 139–147.
- GRAUERT, B., ARNOLD, A. (1968): Deutung diskordanter Zirkonalter der Silvrettadecke und des Gotthardmassives (Schweizer Alpen). *Contr. Mineral. Petrology*, 20, 34–56.
- GRAUERT, B. (1969): Die Entwicklungsgeschichte des Silvretta-Kristallins auf Grund radiometrischer Altersbestimmungen. Ph. D. Thesis, München.
- GRÜNENFELDER, M. (1963): Heterogenität akzessorischer Zirkone und die petrogenetische Deutung ihrer Uran-Blei-Zerfallsalter. I. Der Zirkon des Granodioritgneises von Acquacalda (Lukmanierpass). *SMPM* 43/1, 235–257.
- KELTERBORN, P. (1923): Geologische und petrographische Untersuchungen im Malcantone. *Verh. Natf. Ges. Basel*, 34, 128–230.
- KÖPPEL, V. (1966): Die Vererzungen im insubrischen Kristallin des Malcantone (Tessin). *Beitr. Geol. Schweiz, geotechn. Serie*, 40.
- (1968): Age and history of the uranium mineralization of the Beaverlodge area, Saskatchewan. *Geol. Survey Canada, Paper* 67–31.
- MCDOWELL, F. W. (1970): Potassium-argon ages from the Ceneri zone, Southern Swiss Alps. *Contr. Mineral. Petrology*, 28, 165–182.
- MICHOT, J., DEUTSCH, S. (1969): Les âges U/Pb de zircons et le polycyclisme des gneiss de Brest et des formations encaissantes (Bretagne). *Ann. Soc. Géol. Belgique*, 92, Fasc. II., 263–269.
- PIDGEON, R. T., KÖPPEL, V., GRÜNENFELDER, M. (1970): U-Pb isotopic relationships in zircon suites from a para- and orthogneiss from the Ceneri zone, southern Switzerland. *Contr. Mineral. Petrology*, 26, 1–11.
- RAESIDE, J. D. (1959): Stability of index minerals in soils with particular reference to quartz, zircon and garnet. *J. Sed. Petrology*, 23, 493–502.
- REINHARD, M. (1953): Über das Grundgebirge des Sottoceneri im südlichen Tessin. *Eclogae geol. Helv.* 46/2, 214.
- (1964): Über das Grundgebirge des Sottoceneri im Süd-Tessin und die darin auftretenden Ganggesteine. *Beitr. geol. Karte Schweiz, N.F.* 117.
- SAXENA, S. K. (1966): Evolution of zircons in sedimentary and metamorphic rocks. *Sedimentology* 6, 1–33.
- STAUB, R. (1950): Betrachtungen über den Bau der Südalpen. *Eclogae geol. Helv.* 42/2.
- STEIGER, R. H., WASSERBURG, G. J. (1966): Systematics in the  $\text{Pb}^{208}\text{-Th}^{232}$ ,  $\text{Pb}^{207}\text{-U}^{235}$ , and  $\text{Pb}^{206}\text{-U}^{238}$  systems. *J. Geophys. Research*, 71/24, 6065–6090.
- STERN, T. W., GOLDICH, S. S., NEWELL, M. F. (1966): Effects of weathering on the U-Pb ages of zircon from the Morton gneiss, Minnesota. *E.P.S.L.* 1, 369–371.
- TERMIER, P. (1905): Les Alpes entre le Brenner et la Valtellina. *Bull. Soc. Géol. France* 209–289.